ESCUELA DE CONSTRUCCIÓN CIVIL
FACULTAD DE INGENIERÍA

Revista de la Construcción
Journal of Construction

Research Article

Response surface optimization of geopolymer mix parameters in terms of key engineering properties

Şevin Ekmen[1]*, Kasım Mermerdaş[2] Zeynep Algın[3], Yusuf Işıker[4]

[1] Department of Civil Engineering, Harran University, Şanlıurfa (Türkiye), ekmensevin@harran.edu.tr
[2] Department of Civil Engineering, Harran University, Şanlıurfa (Türkiye), kasim.mermerdas@harran.edu.tr
[3] Department of Civil Engineering, Harran University, Şanlıurfa (Türkiye), zyilmaz@harran.edu.tr
[4] Department of Mechanical Engineering, Harran University, Şanlıurfa (Türkiye), yusuf47@harran.edu.tr
*Correspondence: ekmensevin@harran.edu.tr

Received: 27.09.2021; **Accepted:** 09.12.2022; **Published:** 29.12.2022

Citation: Ekmen, S., Mermerdaş, K., Algın, Z. and Işıker, Y. (2022). Response surface optimization of geopolymer mix parameters in terms of key engineering properties. Revista de la Construcción. Journal of Construction, 21(3), 631-644. https://doi.org/10.7764/RDLC.21.3.631.

Abstract: The main aim of the current study is to search the impact of variable matrix phase features on fly ash based lightweight geopolymer mortars (LWGM). Another scope of the study is to obtain performance oriented optimum mixture proportions through response surface method (RSM). In order to have low unit weight for LWGMs, pumice aggregate was utilized as a part of the aggregate. The investigated engineering properties are water absorption, drying shrinkage and thermal conductivity. By performing optimization analysis, it was aimed to obtain the best numerical models representing the experimental results depending on the input variables. The decrease of liquid (alkali activators) to powder (fly ash) ratio, Na_2SiO_3 solution to NaOH solution ratio and increase of sodium hydroxide molarity led to improvement of compressive strength. Dry thermal conductivity values in dry state were observed to be less than those of saturated ones. Moreover, the higher sodium hydroxide molarity and lower Na_2SiO_3 solution to NaOH solution ratios, and liquid to powder ratios resulted in further shrinkage reduction. Depending on the goals of maximum compressive strength, minimum water absorption, and drying shrinkage, optimum values for molarity, SS/SH, and l/p factors were determined as 14 M, 1.586, and 0.45, respectively.

Keywords: Geopolymer, water absorption, drying shrinkage, thermal conductivity, optimization.

1. Introduction

The ordinary Portland cement (OPC) consumption at high rates in the construction industry as the main binding material results in excessive usage of natural material and hence some environmental issues. The research exhibit that the manufacturing process of a ton of cement releases nearly one ton of CO_2 gas to the atmosphere (Li et al., 2011; Peng et al., 2013). Thereby, the OPC production is responsible for the 7-8% of the released CO_2 in the atmosphere (Huntzinger & Eatmon, 2009; Meyer, 2009; Ekmen et al., 2020). The investigations on alternative binder materials to mitigate this problem has attracted the interests of researchers for decades. Alternative materials such as metakaolin, red mud, industrial wastes, such as, blast

furnace slag, fly ash, silica fume, etc. have been utilized for their potential to substitute cement as supplementary cementing materials. Moreover, they have also been used in the manufacture of pozzolanic or composite cements to overcome the high OPC demand to avoid from its disadvantages. The geopolymer technology leads consumption of the solid residues and accordingly contributes to disposal or the storage problem of these wastes.

In the geopolymerization process, 3-dimensional polymeric Si–O–Al–O bonds occur due to the reaction of alkali activators (alkali hydroxide, alkali silicate) and aluminosilicate-based powder sources. The need to investigate the effects of the aforementioned parameters has promoted intensive research on the mechanical, durability, absorption, and microstructural behavior of geopolymers (Amran et al., 2020; Duxson et al., 2007; Hardjito et al., 2004; Kaya & Köksal, 2021; Shi et al., 2020; Zhang et al., 2018)

There is an ongoing interest in using various lightweight aggregates in structural or nonstructural materials thanks to the advantages such as low dead weight, better thermal insulation, fire resistance, and lower transportation cost (Mouli & Khelafi, 2008). Pumice aggregate (PA) is a lightweight aggregate containing a porous structure and a density lower than 1 gr/cm^3. Due to the formation stage, the structure of the volcanic aggregate contains bubbles with different shapes such as interconnected or elongated. The highest pumice aggregate deposits in the world are available in Turkey, Italy, and Greece. Turkey deposits comprise 31.7% of the lightweight aggregate reserves in the world (Razak et al., 2015; Sarmin, 2015). When the literature studies were examined, it was noticed that the studies about optimization of pumice-based lightweight geopolymer mortars are limited considering various mix proportions and the matrix parameters (Wongsa et al. 2018). It is important to determine the optimum mixture proportions of mixtures without trial studies. Hence, in this study it was adopted to contribute to completing the gap with optimization study on pumice based lightweight geopolymer mortar. A comprehensive experimental investigation was conducted on the pumice aggregate-based lightweight geopolymer mortar considering various mix proportions. Engineering properties of the mortars were evaluated through compressive strength, water absorption, shrinkage and thermal conductivity. The chief investigation parameters were the effectiveness of different liquid to powder ratios (l/p), sodium hydroxide molarities, and sodium silicate to sodium hydroxide ratios.

2. Materials and methods

2.1. Materials

In this experimental program, the materials of fly ash, sodium silicate, sodium hydroxide, river sand, and pumice aggregate, and superplasticizer were utilized to make LWGM mixes.

The lightweight pumice aggregate is a volcanic material, and it was supplied from Nevşehir city in Turkey. Due to the fast-cooling formation stage of the basaltic pumice aggregate, it contains bubbles and voids, so it has a porous and rough texture. It is an inert material with a pH value of around 7. The pumice aggregate which is used with saturated surface dry (SSD) condition in this study is a natural lightweight aggregate that has a specific gravity of 1.2 and, 26% water absorption value. A regionally located river sand was employed in the fine aggregate mix. The sieve analysis results of the fine aggregates were illustrated in Table 1 together with lower and upper limits specified in ASTM C33 standard (ASTM:C33-03, 2003).

Table 1. Sieve analysis of the used aggregates.

Sieve size	Upper limit	Lower limit	River sand	Pumice aggregate
4.75	100	95	99.8	100
2.36	100	80	94.3	85.1
1.18	85	50	56.3	65.4
0.6	60	25	27.0	36.2
0.3	30	5	7.5	22
0.15	10	0	2.6	0

The composition of FA was attained by X-ray fluorescence analysis. FA was obtained from the Çatalağzı thermal power

plant in Turkey. Chemical constituents of the FA are 55.46% SiO_2, 26.33% Al_2O_3, 6.71% Fe_2O_3, 1.69% CaO, 2.42% MgO, 1.08% Na_2O, 4.22% K_2O, 0.1% Cl-, and loss on ignition (LOI) value is determined to be 1.2%. The total amount of the three main elements of Al_2O_3, SiO_2, and Fe_2O_3 is higher than 70% of the oxides in the fly ash. Hence, the used FA in this experimental study is with conformity ASTM C-618 standard (American Society for Testing and Materials, 1997). Another important physical property of FA, namely, the specific surface area determined by BET analysis and found to be 2.02 m^2/g. The specific gravity value was measured as 2.

To prepare the alkaline solutions, the following procedure was carried out. One liter of NaOH (SH) solutions were prepared by mixing the 400, 480, and 560 g NaOH pellets with required amount of distilled water to get 10 M, 12 M, and 14 M target sodium hydroxide molarities, respectively. Since the dissolution of sodium hydroxide pellets in water is an exothermic phenomenon, NaOH solutions were prepared by gradual addition of water in the beaker until ambient heat balance is provided. After that, the prepared solutions with different molarities were kept in the laboratory in closed tubes at room temperature until casting of LWGMs. The sodium silicate solution (water glass) which has SiO_2/Na_2O ratio of 2.5 with a specific gravity of 1.38 was supplied from a local company. Considering the aim of providing sufficient workability, a superplasticizer with a specific gravity of 1.07 was also exploited in the present study.

2.2. Mixture design and casting procedure

The mix design parameters of the study were determined to search the transport and thermal properties of pumice-based geopolymer mortars with various SS to SH ratios, sodium hydroxide molarities, and l/p ratios. For this purpose, eighteen mixtures were prepared considering three SS to SH ratios of 2.5, 2, 1.5, three sodium hydroxide concentrations of 10 M, 12 M, 14 M, and two l/p ratios of 0.45, 0.55 to produce LWGM samples. The mixture proportions of LWGMs were presented in Table 2. Total aggregate is composed of 65% river sand and 35% pumice aggregate by volume. Through the preliminary study, it was proved that the usage of the porous pumice aggregate at high rates, resulted in a significant reduction in the compressive strength of LWGMs. Hence, this replacement amount (35%) was adopted to realize the aim of obtaining lightweight mortar of sufficient compressive strength. SP amount was determined as 1.5% of fly ash content. The flow diameters measured according to ASTM C 1437 were determined to be 25±3 cm.

Table 2. Mix proportions of LWGM mixtures.

Liquid/powder	SS/SH ratio	Sodium hydroxide (Molarity, M)	Sodium silicate (kg/m^3)	Sand (kg/m^3)	Pumice aggregate (kg/m^3)	Superplasticizer (kg/m^3)
0.45	2.5	10	188.42	888	228	9.4
		12	188.42	893	230	9.4
		14	188.42	897	231	9.4
	2	10	175.86	887	228	9.4
		12	175.86	892	229	9.4
		14	175.86	897	231	9.4
	1.5	10	158.28	885	228	9.4
		12	158.28	891	229	9.4
		14	158.28	897	231	9.4
0.55	2.5	10	215.44	873	225	8.8
		12	215.44	878	226	8.8
		14	215.44	883	227	8.8
	2	10	201.08	872	224	8.8
		12	201.08	877	226	8.8
		14	201.08	883	227	8.8
	1.5	10	180.97	869	224	8.8
		12	180.97	876	225	8.8
		14	180.97	883	227	8.8

To make the dry materials ready, FA was mixed with a previously prepared fine aggregate mixture consisting of pumice aggregate and river sand for a total of five minutes using a laboratory-type mixer. Then, the mixture of SS and SH solutions which had been kept in ambient condition to allow heat balance before starting the casting process, and superplasticizer were slowly added to the dry materials, and the mixing operation was continued for 5 more minutes. The same mixing procedure was applied for all mixtures. After completion of the process, the fresh mixtures are poured into suitable molds to be used for the experiments. The prepared mixtures were compacted in the molds through a vibrating table. The vibration period and frequency are thoroughly adjusted to assure both full compaction and no segregation. Improper compaction results in a rise of the pumice aggregate particles to the surface. So, this causes non-homogeneity of the mix. As soon as the compaction is completed, the samples are kept at room temperature for approximately 1-2 hours. Later, they are covered with plastic bags and kept in the oven under 75 ºC for 24 hours. After the demolding process, the specimens are kept in ambient laboratory condition until test time.

2.3. Test procedure

The compressive strength values of LWGMs at 28th days were determined in a previous study of the authors (Ekmen et al. 2021) using 50x50x50 mm samples conforming to ASTM C109/C109M-16a (ASTM C109/C109M-02, 2005). In the current study the test results were benefited for optimization. For water absorption measurement, three cubic specimens with 50 mm dimensions were kept in the ambient temperature before the testing time of 28 days according to ASTM C642-13 (American Society of Testing and Materials, 2006). In this study, the drying shrinkage measurement was conducted with 25×25×285 mm samples according to the C596-09 (ASTM 2009b) (ASTM C596–01, 2001).

The thermal conductivity test was performed using three 50x50x50 mm cubes for each mix by TPS 500 S Hot Disk Thermal Constants Analyzer with a single-sided method according to ISO 22007-2 (Özen et al., 2022, Zheng et al., 2020). This method is a disc heat source-based method (Işıker, 2018). Two different methods were used in thermal conductivity measurements. The test was conducted for both dry and water-saturated condition of samples.

3. Experimental results and analysis

3.1. Compressive strength

Figure 1 demonstrates the 28-day compressive strength results of LWGMs for l/p:0.45 and l/p:0.55 obtained. The effects of various sodium silicate to sodium hydroxide ratios, sodium hydroxide molarities, and the ratio of liquid to powder on the compressive strength development of the samples can be seen from Figure 1. The increase of sodium hydroxide molarity provided higher compressive strength results for all mixes. The highest compressive strength development was generally obtained when sodium hydroxide concentration increased from 12 M to 14 M. The decrement of Na_2SiO_3 to NaOH ratio facilitate to compressive strength improvement due to the negative effect of the excess Si amount on the geopolymerization reaction. The variation of the liquid to powder ratio from 0.45 to 0.55 reduced the obtained compressive strength results. The conclusion can be with respect to the higher H_2O content in the specimens with the ratio of liquid to powder of 0.55 and accordingly more porous structure. The detailed information and the discussion of compressive strength results can be found in a previous study by Ekmen et al. (2021).

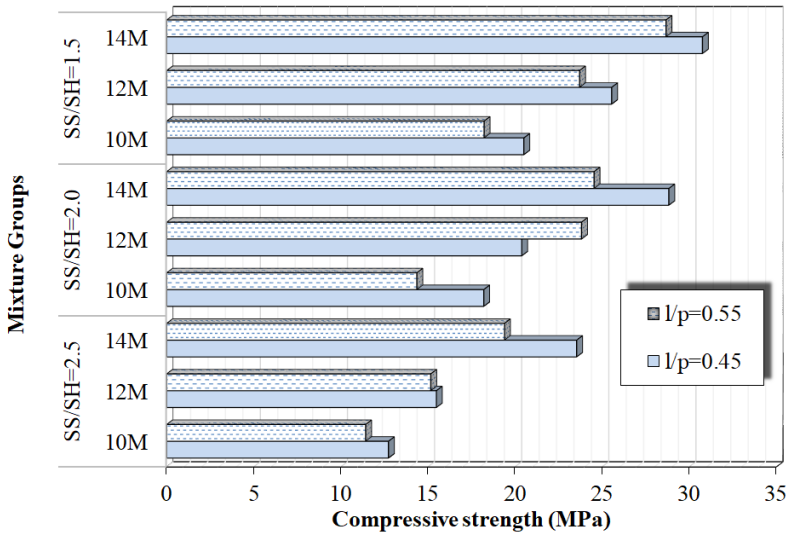

Figure 1. Compressive strength results of the LWGMs for l/p: 0.45 and, l/p: 0.55 (*adapted from authors' previous study Ekmen et al. 2021*).

3.2. Water absorption

Figure 2 illustrates the water absorption values for LWGMs with various SS to SH ratios according to sodium hydroxide molarities at age of 28-day. The trends of the curves in Figure 2a and Figure 2b represent the relations for the liquid to powder ratios of 0.45 and 0.55, respectively. While the water absorption results varied between 7.61-11.96 (%) at the liquid to powder ratio of 0.45, the range was obtained as 9.96-13.59 (%) at the liquid to powder ratio of 0.55. The water absorption values increased with the high degree of alkalinity. The increase of sodium hydroxide concentration resulted in a decrease in water absorption values for the both liquid to powder ratios. The obtained relation can be attributed to the formation of a denser matrix and accordingly, diminishing the void content. When Figure 2a examined, it was seen that the rate of water absorption was decreased with the reduction of the sodium silicate to sodium hydroxide ratios at SH molarities of 12 M and 14 M. The highest decline in water absorption of 1.98% was observed with the decrease of sodium silicate to sodium hydroxide ratio from 2.5 to 2 at sodium hydroxide concentration of 10 M. In Figure 2b the SS to SH ratio reduction led to decrease of water absorption results at all sodium hydroxide molarities. Besides, the alteration of Na_2SiO_3 to NaOH ratio from 2 to 1.5 has no significant effect on the water absorption values at sodium hydroxide molarities of 12 M and 14 M. The highest water absorption decrease of 1.47% was reached with the decline of sodium silicate to sodium hydroxide ratio from 2.5 to 2 at 10 M sodium hydroxide molarity.

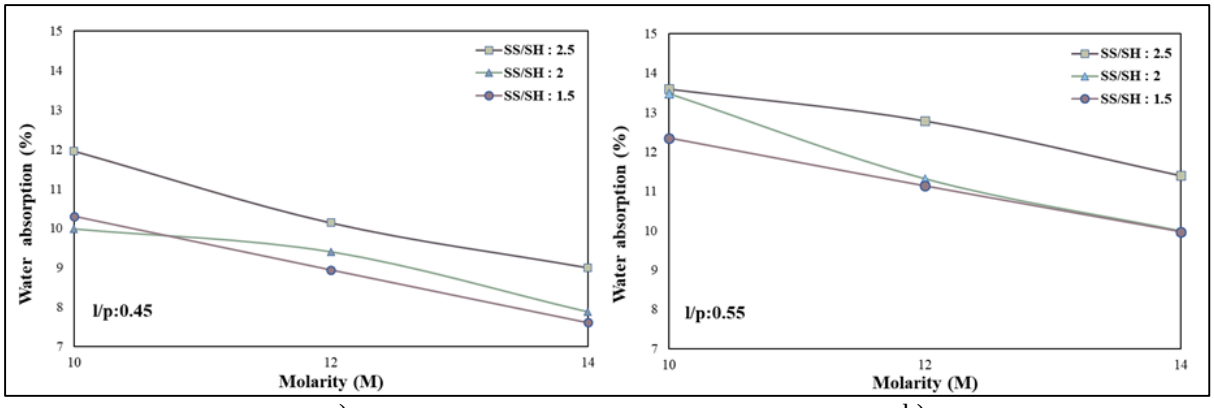

a) b)

Figure 2. Water absorption results for a) l/p:0.45 ratio and b) l/p:0.55 ratio.

3.3. Shrinkage

Figure 3 illustrates the effects of the various SS to SH ratios sodium hydroxide molarities and the ratios of liquid to powder on the drying shrinkage values of LWGMs over 90-days of drying period. As seen in Figure 3, about 80 percent of drying shrinkage results can be reached within 3 weeks. When the obtained data were interpreted it was also concluded that the drying shrinkage values of LWGMs decreased as the sodium hydroxide molarity increased regardless of the SS to SH ratios and the ratios of liquid to powder. However, the fluctuation level varied according to the two parameters. For instance, when sodium hydroxide molarity increased from 10 M to12 M the highest drying shrinkage increment value of 44.4% was obtained with SS to SH ratio of 2.5 and the liquid to powder ratio of 0.45.

However, considering the variation of NaOH concentration from 12 M to 14 M, the maximum shrinkage of 52.9% was observed with the sodium silicate to sodium hydroxide ratio of 2 and liquid to powder ratio of 0.55. This inevitable finding attributes to the improvement of the geopolymerization reaction and so volume stability. Similar results were reported by the other researchers (Aydin & Baradan, 2014; Atiş et al., 2009; Jiao, Wang, Zheng, & Huang, 2018). Overall, it was clear that the reduction in the sodium silicate to sodium hydroxide ratio resulted in the lower the shrinkage values in all mixtures, but higher increment levels were obtained when SS to SH ratio changed from 2 to 2.5.

In the case of the liquid to powder ratio of 0.45, when SS to SH ratio increased from 2 to 2.5, the ultimate shrinkage increments of 35.75%, 35.4%, and 55.4% were attained with mixtures containing 10 M, 12 M, and 14 M sodium hydroxide molarities, respectively. Regarding the mixtures containing liquid to powder ratio of 0.55, the above-mentioned values were determined as 22%, 63.4%, and 43%, respectively.

When Figure 3 was examined, it was found that the increase of the l/p ratio from 0.45 to 0.55 caused higher drying shrinkage results at varying rates regarding to the various SS to SH ratios and sodium hydroxide molarities. Considering the increase in the ratio of liquid to powder, the highest drying shrinkage rise of 33.4% was obtained with the mix containing sodium silicate to sodium hydroxide of 2 and 14 M sodium hydroxide molarity.

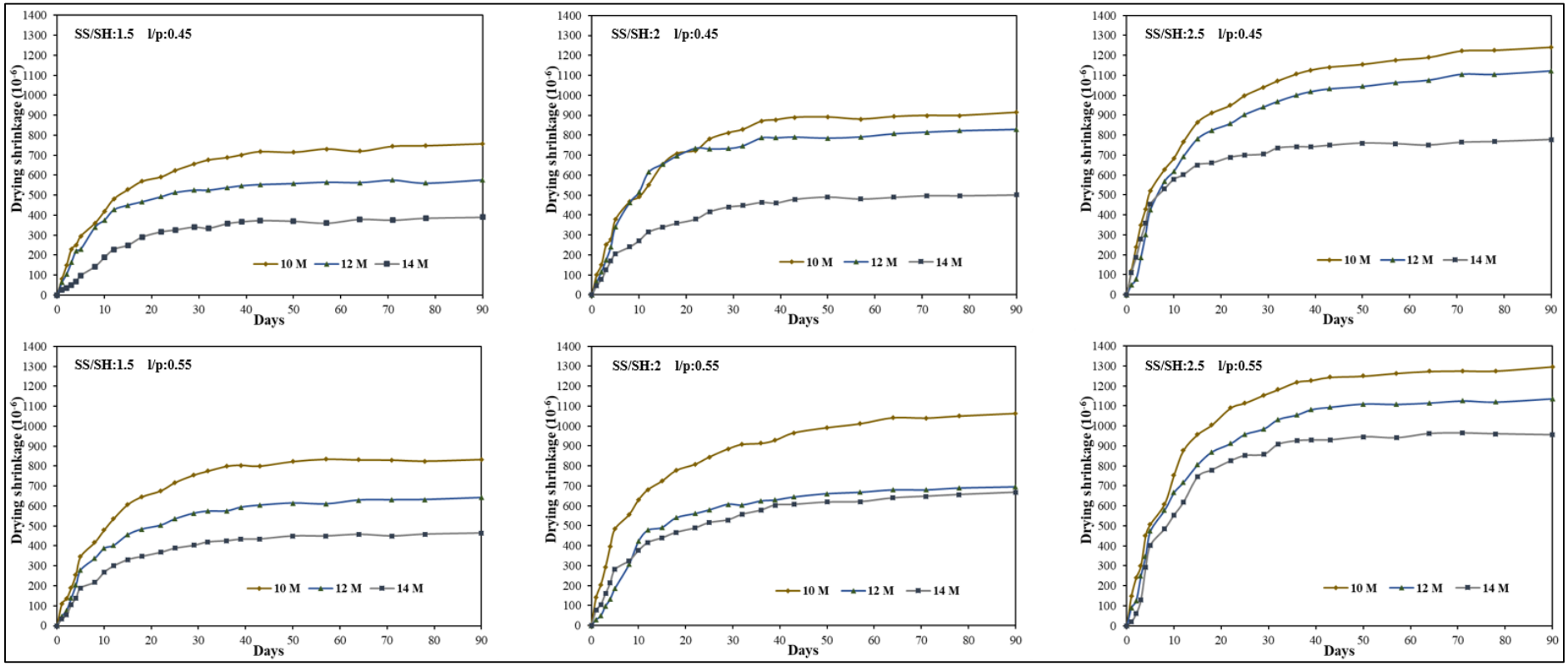

Figure 3. Drying shrinkage results of LWGMs according to sodium silicate to sodium hydroxide ratios, sodium hydroxide molarities and liquid to powder ratios.

3.4. Thermal conductivity

Thermal performance of the concrete is important for carbon emission of buildings. Thermal characteristics of building materials have a considerable influence on the carbon emission in the building operation stage since this stage of a building's life contributes between 50 and 70% of its overall carbon emissions (Hao et al., 2022). 40% of annual worldwide carbon emissions come from the built environment. Building operations account for 27% of the total yearly cost, while construction and infrastructure materials accounts for another 13%. Concrete with low thermal conductivity decreases heat loss through walls in building structures [Dai et al., 2022]. In order to minimize heat, transfer and energy consumption in building constructions, low thermal conductivity concrete can be used.

Figure 4 shows the thermal conductivity results for saturated and dry conditions of LWGMs according to the various mix parameters. As expected, the thermal conductivity values of samples in saturated conditions are higher than the samples in dry conditions. The molarity increment resulted in higher thermal conductivity values for all mixes but with different degrees. The highest thermal conductivity variation was determined for the mixes with Na_2SiO_3 to NaOH ratio of 2, when the NaOH concentration increased from 10 M to 12 M. In general, the rise of the l/p ratio from 0.45 to 0.55 facilitated thermal conductivity decrease due to causing a higher pore structure. When the impact of the sodium silicate to sodium hydroxide ratio on the thermal conductivity results was examined, it was concluded that there is no obvious trend that represents the relation between the two parameters.

The influence of the SS to SH ratio varied according to the sodium hydroxide concentration and liquid to powder ratio variation. The range of thermal conductivity values of the samples corresponding to the various SS to SH ratios, sodium hydroxide molarities, and the ratios of liquid to powder were measured as 0.54-0.79 W/mK and 0.81-1.33 W/mK at the dry and saturated condition of samples, respectively. The minimum thermal conductivity values of saturated and dry conditions were determined as 0.81 W/mK and 0.54 W/mK in the samples with the ratio of liquid to powder of 0.55 and sodium hydroxide molarity of 10 M, respectively. This study revealed that low molarity and dry concretes are more efficient in terms of carbon emissions due to their low thermal conductivity. In addition, the best concrete for energy consumption occurred in SS/SH:2 type.

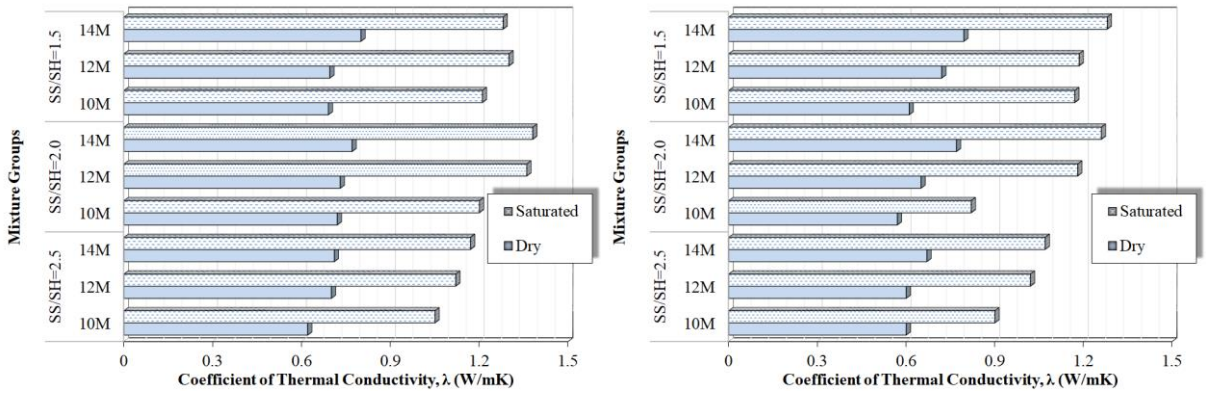

Figure 4. The coefficient of thermal conductivity values of LWGMs according to the various mix parameters; a) l/p=0.45 and b) l/p=0.55

3.5. Optimization

Design-Expert (2010) software was used in the multi-objective optimization analysis carried out within the scope of this research. Central composite design, which is the most widely used design method, was chosen to find the functional relationship between responses and inputs. SH molarity values, SS/SH, and l/p ratios were considered as input variables and optimum values were determined for output parameters of water absorption, compressive strength, thermal conductivity, and drying shrinkage test results of fly ash-based lightweight geopolymer mortars. With this optimization analysis, it is aimed to obtain the best models representing the experimental results depending on the independent input variables. These models were created using the response surface method, which is a combination of statistical and mathematical approaches. As a result, the

SS/SH, l/p ratios, and SH molarity values that provide the maximum compressive strength, minimum water absorption, minimum drying shrinkage values of fly ash-based lightweight geopolymer mortars has been reached. Multivariate regression analyzes were performed using high order polynomial models for each response. A stepwise backward selection algorithm was used to abbreviate the terms of models, and statistically significant model terms were determined by analysis of variance. In addition, the exponential transformation was applied to these models of water absorption, compressive strength, thermal conductivity, and drying shrinkage responses in order to improve the analysis results.

Formulations achieved from the regression analysis which is executed for compressive strength, water absorption, thermal conductivity, and drying shrinkage responses, and the applied exponential transformation are given in (Equation 1-4). The terms used in these equations, the coefficient values of these terms, and the results obtained from the variance analysis for each output are summarized in Table 3. The p values of the compressive strength, water absorption, thermal conductivity, and drying shrinkage response models are less than 0.05, which proves that the models representing the relationship between input and output parameters are statistically significant.

Table 3. The coefficients given in Eqs. (1-4) and analysis of variance outputs depending on the regression analysis for water absorption, compressive strength, thermal conductivity, and drying shrinkage.

Corresponding response	Factor	Coefficient	Statistical assessment						
			SS	Degree of freedom	MS	F value	p-value	Contribution (%)	Significance
Compressive strength (MPa)	Model	c_1=148.20235	33.5	7	4.79	57.38	<0.0001	-	Yes
	A-l/p	c_2=296.98021	0.016	1	0.016	0.2	0.6682	0.05	No
	B-SS/SH	c_3=3.36198	12.83	1	12.83	153.81	<0.0001	38.4	Yes
	C-Molarity	c_4=24.51643	18.55	1	18.55	226.36	<0.0001	55.51	Yes
	AC	c_5=50.05407	0.018	1	0.018	0.21	0.6551	0.05	No
	B^2	c_6=1.35750	0.46	1	0.46	5.52	0.0406	1.38	Yes
	C^2	c_7=1.05542	$1.369x10^{-3}$	1	$1.369x10^{-3}$	0.016	0.9006	0	No
	AC^2	c_8=2.10158	0.71	1	0.71	8.47	0.0155	2.12	Yes
	Residual		0.83	10	0.083			2.48	-
Water absorption (%)	Model	a_1=4.14103	2.83	4	0.71	150.73	<0.0001	-	Yes
	A-l/p	a_2=5.40288	1.31	1	1.31	279.74	<0.0001	45.31	Yes
	B-SS/SH	a_3=1.27223	0.33	1	0.33	70.47	<0.0001	11.41	Yes
	C-Molarity	a_4=0.15454	1.15	1	1.15	244.12	<0.0001	39.78	Yes
	B^2	a_5=0.40109	0.04	1	0.04	8.56	0.0118	1.38	Yes
	Residual		0.061	13	$4.696x10^{-3}$			2.11	Yes
Thermal conductivity (W/mK)	Model	b_1=0.52536	0.12	3	0.038	18.56	<0.0001	-	Yes
	A-l/p	b_2=0.67684	0.021	1	0.021	9.97	0.007	14.48	Yes
	B-SS/SH	b_3=0.098061	0.029	1	0.029	13.95	0.0022	20	Yes
	C-Molarity	b_4=0.036993	0.066	1	0.066	31.76	<0.0001	45.52	Yes
	Residual		0.029	14	$2.068x10^{-3}$			20	Yes
Drying shrinkage. (10^{-6})	Model	d_1=3627.78543	32914.95	7	4702.14	80.98	<0.0001	-	Yes
	A-l/p	d_2=7822.01811	12.55	1	12.55	0.22	0.652	0.04	No
	B-SS/SH	d_3=92.26683	18440.69	1	18440.69	317.57	<0.0001	56.15	Yes
	C-Molarity	d_4=665.36748	12752.55	1	12752.55	219.61	<0.0001	38.83	Yes
	AC	d_5=1331.51049	63.59	1	63.59	1.1	0.32	0.19	No
	B^2	d_6=42.66724	455.12	1	455.12	7.84	0.0188	1.39	Yes
	C^2	d_7=28.88240	28.13	1	28.13	0.48	0.5023	0.09	No
	AC^2	d_8=56.43880	509.65	1	509.65	8.78	0.0142	1.55	Yes
	Residual		580.68	10	58.07			1.77	-

SS: Sum of squares, MS: Mean of squares

$$\text{Compressive strength} = (c_1 - c_2A + c_3B - c_4C + c_5AC - c_6B^2 + c_7C^2 - c_8AC^2)^{\frac{1}{0.67}} \quad \text{(Eq.1)}$$

$$\text{Water absorption} = (a_1 + a_2A - a_3B - a_4C + a_5B^2)^{\frac{1}{0.6}} \quad \text{(Eq.2)}$$

$$\text{Thermal conductivity} = (a_1 - a_2A - a_3B + a_4C)^{\frac{1}{2.22}} \quad \text{(Eq.3)}$$

$$\text{Drying shrinkage} = (-d_1 + d_2A - d_3B + d_4C - d_5AC + d_6B^2 - d_7C^2 + d_8AC^2)^{\frac{1}{0.77}} \quad \text{(Eq.4)}$$

Three-dimensional response surface graphs for compressive strength, water absorption, thermal conductivity, and drying shrinkage models (Equation 1-4.) were given in Figure 5, 6, 7 and 8. Figure 5, 6, 7 and 8. show the effects of SH molarity, SS/SH, and l/p ratios on compressive strength, water absorption, thermal conductivity, and drying shrinkage responses.

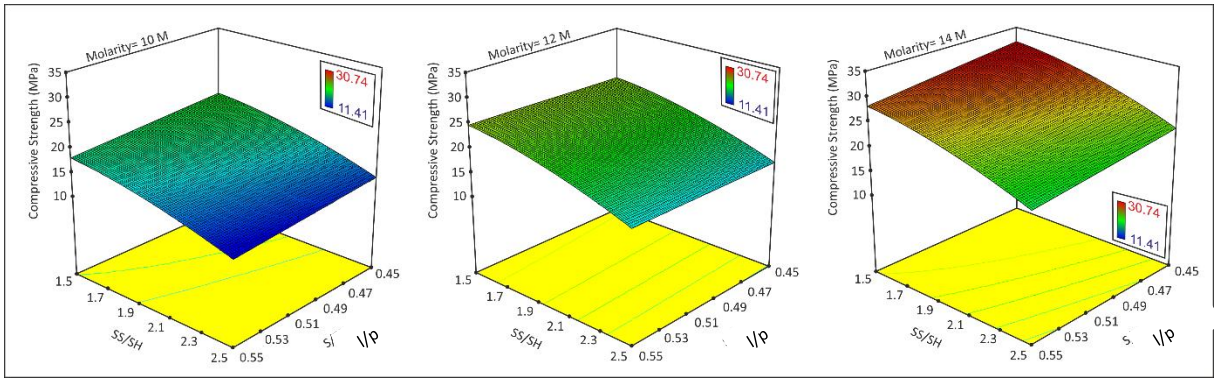

Figure 5. Three-dimensional representation of the response surface model for compressive strength

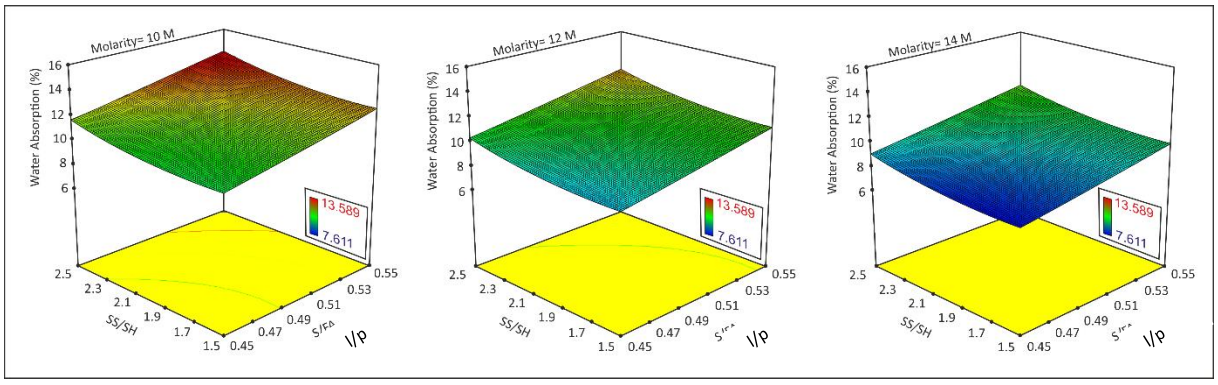

Figure 6. Three-dimensional representation of the response surface model for water absorption.

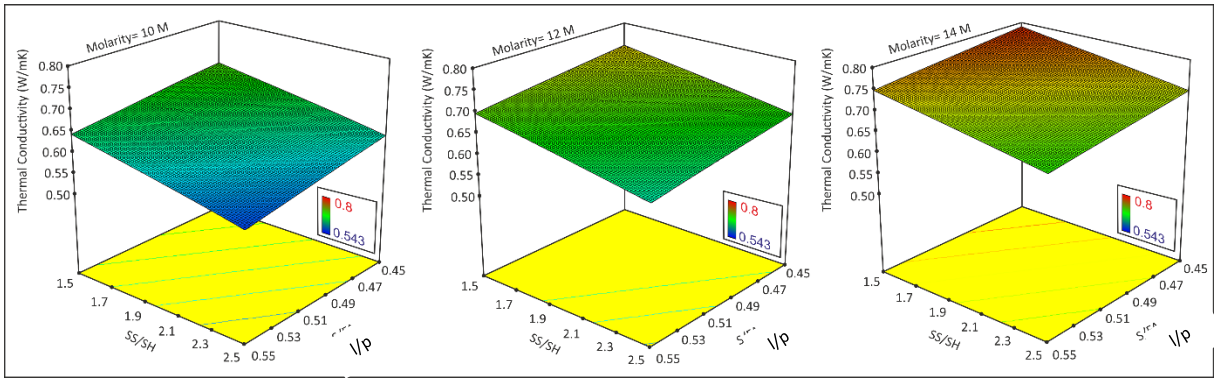

Figure 7. Three-dimensional representation of the response surface model for thermal conductivity.

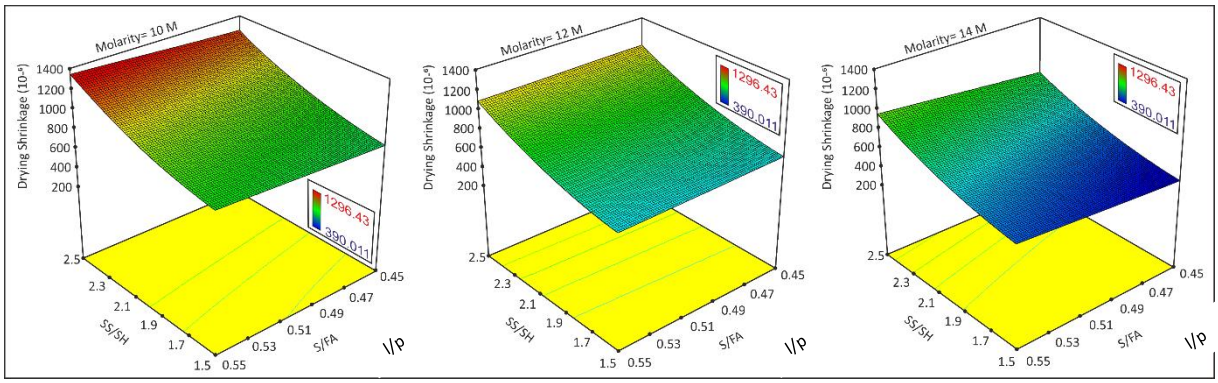

Figure 8. Three-dimensional representation of the response surface model for drying shrinkage

In this study, the response surface method determines the relationship between factors such as molarity, SS/SH, and l/p ratios and responses, as well as to reach the combined effect of the factors on the properties of lightweight geopolymer mortars and to achieve the optimum SS/SH, l/p and SH molarity values that give the maximum compressive strength, minimum water absorption and drying shrinkage values. Figure 9 illustrates the alteration of the desirability approach obtained from the optimization study performed on compressive strength, water absorption, thermal conductivity, and drying shrinkage responses. The data gained from the optimization analysis using the response surface method is presented in Table 4. Optimum values for molarity, SS/SH, and l/p factors were determined as 14 M, 1.586, and 0.45, respectively, depending on the goals of maximum compressive strength, minimum water absorption, and drying shrinkage. The desirability value of this optimization analysis was obtained as 0.996.

Table 4. The obtained findings from the optimization investigation

Input and output factors	Optimum and predicted output values
l/p	0.45
SS/SH	1.586
Molarity (M)	14
Compressive strength (MPa)	31.519
Water absorption (%)	7.689
Thermal conductivity (W/mK)	0.784
Drying shrinkage (10^{-6})	379.3
Desirability	0.996

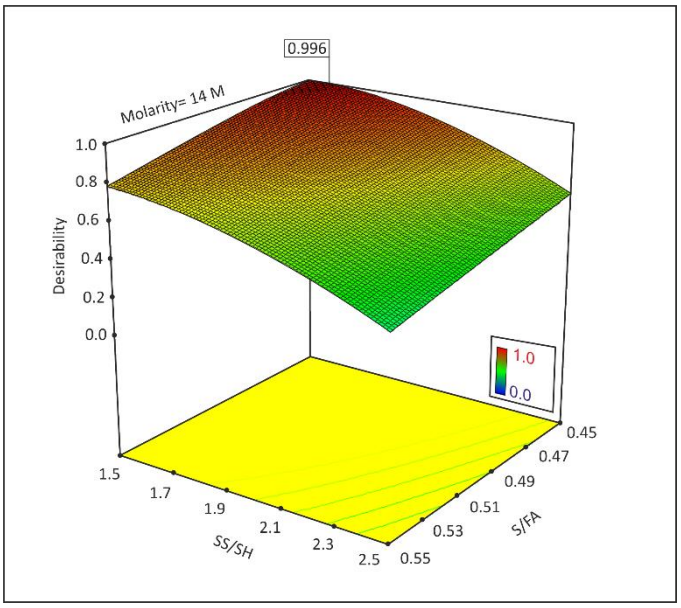

Figure 9. Three-dimensional graphical representation of the desirability function obtained from optimization analysis.

4. Conclusions and comments

The study aims to determine some critical engineering properties of LWGMs and optimizing the data obtained from laboratory study. The conclusions drawn can be given as follows:

1. At higher sodium hydroxide concentration and lower SS to SH ratio, significant enhancement regarding the engineering properties of LWGMs were observed as a result of the improved development of geopolymerization reaction.
2. Lower absorption characteristics were achieved at the liquid to powder ratio of 0.45 mainly depending on the molarity of the NaOH solution and SS/SH ratio. The LWGMs water absorption values seemed to be more sensitive to the change in l/p ratio than molarity and SS/SH ratio.
3. The shrinkage behavior of LWGMs is directly affected from l/p ratio. The higher l/p ratio the higher the shrinkage is. However, the molarity of the mixes seemed to be more dominant due to the effect on the geopolymerization and hence stiffness and porosity of the material.
4. The range of thermal conductivity values of the samples were seemed to have similar values for cement based conventional mortars (0.7-1.3 W/mK). However, in some instances, especially for dry case measurement, the coefficient of thermal conductivity values was observed to relatively lower than conventional mortars.
5. The obtained experimental findings were utilized to perform response surface-based optimization modelling of the critical mix parameters. The obtained desirability of optimization by means of the maximization of compressive strength, and minimization water absorption, and drying shrinkage was 0.996. Depending on the aforementioned goals optimum values for molarity, SS/SH ratio, and l/p parameters were determined as 14 M, 1.586, and 0.45, respectively.

Author contributions: ŞE; Data processing, experimental study, writing, revising. KM; Conceptualization, writing, revising. ZA; Data processing, writing. YI; Experimental study.

Funding: The authors would like to thank Harran University Scientific Research Projects Coordination Unit (HÜBAP) for financial support under grant number 18252. Project Name: "Investigating, Modelling and Optimization of Fresh and Hardened Properties of Fly Ash Based Lightweight Geopolymer Mortars" (In Turkish).

Conflicts of interest: The authors declare no conflict of interest.

References

Akcay, C., & Manisali, E. (2018). Fuzzy decision support model for the selection of contractor in construction works. Revista de la Construcción. Journal of Construction, 17(2), 258-266.

American Society for Testing and Materials. (1997). ASTM C 618 : Standard specification for coal fly ash and raw or calcined natural pozzolan for use as a mineral admixture in concrete. Annual Book of ASTM Standards.

American Society of Testing and Materials. (2006). ASTM C642 Standard test method for density, absorption, and voids in hardened concrete. ASTM International, (3).

Amran, Y. H. M., Alyousef, R., Alabduljabbar, H., & El-Zeadani, M. (2020). Clean production and properties of geopolymer concrete; A review. Journal of Cleaner Production. doi:10.1016/j.jclepro.2019.119679

ASTM C109/C109M-02. (2005). Standard test method for compressive strength of hydraulic cement mortars. Annual Book of ASTM Standards.

ASTM C1437-01 (2001) Standard test method for flow of hydraulic cement mortars, Annual Book of ASTM Standards, Philadelphia, 04.01.2005, pp. 611–612.

ASTM C596–01. (2001). Standard test method for drying shrinkage of mortar containing hydraulic cement. Annual Book of ASTM Standards, 2(4).

ASTM:C33-03. (2003). Standard specification for concrete aggregates. ASTM International.

Aydin, S., & Baradan, B. (2014). Effect of activator type and content on properties of alkali-activated slag mortars. Composites Part B: Engineering, 57. doi:10.1016/j.compositesb.2013.10.001

Dai, J., Wang, Q., Bi, R., Wang, C., Han, Z., Du, W., & Chen, Z. (2022). Research on influencing factors and time-varying model of thermal conductivity of concrete at early age. Construction and Building Materials, 315, 125638. doi: 10.1016/j.conbuildmat.2021.125638

Duran Atiş, C., Bilim, C., Çelik, Ö., & Karahan, O. (2009). Influence of activator on the strength and drying shrinkage of alkali-activated slag mortar. Construction and Building Materials, 23(1). doi:10.1016/j.conbuildmat.2007.10.011

Duxson, P., Fernández-Jiménez, A., Provis, J. L., Lukey, G. C., Palomo, A., & van Deventer, J. S. J. (2007). Geopolymer technology: The current state of the art. Journal of Materials Science, 42(9). doi:10.1007/s10853-006-0637-z

Ekmen, A. B., Algin, H. M., & Özen, M. (2020). Strength and stiffness optimisation of fly ash-admixed DCM columns constructed in clayey silty sand. Transportation Geotechnics, 24. doi:10.1016/j.trgeo.2020.100364

Ekmen, Ş., Mermerdaş, K., & Algın, Z. (2021). Effect of oxide composition and ingredient proportions on the rheological and mechanical properties of geopolymer mortar incorporating pumice aggregate. Journal of Building Engineering, 34, 101893.

Hao, L., Xiao, J., Sun, J., Xia, B., & Cao, W. (2022). Thermal conductivity of 3D printed concrete with recycled fine aggregate composite phase change materials. Journal of Cleaner Production, 364, 132598. doi: 10.1016/j.jclepro.2022.132598

İşıker, Y. (2018). Development of an experimental method for determination of thermal performances of energy efficient alternative building materials. PhD Thesis, Harran University, Sanlıurfa.

Hardjito, D., Wallah, S. E., Sumajouw, D. M. J., & Rangan, B. V. (2004). On the development of fly ash-based geopolymer concrete. ACI Materials Journal, 101(6). doi:10.14359/13485

Huntzinger, D. N., & Eatmon, T. D. (2009). A life-cycle assessment of Portland cement manufacturing: comparing the traditional process with alternative technologies. Journal of Cleaner Production, 17(7). doi:10.1016/j.jclepro.2008.04.007

Jiao, Z., Wang, Y., Zheng, W., & Huang, W. (2018). Effect of dosage of sodium carbonate on the strength and drying shrinkage of sodium hydroxide based alkali-activated slag paste. Construction and Building Materials, 179. doi:10.1016/j.conbuildmat.2018.05.194

Kaya, M., & Köksal, F. (2021). Influences of high temperature on mechanical properties of fly ash based geopolymer mortars reinforced with PVA fiber. Revista de La Construcción, 20(2). doi:10.7764/RDLC.20.2.393

Li, C., Gong, X., Cui, S., Wang, Z., Zheng, Y., & Chi, B. (2011). CO_2 emissions due to cement manufacture. In Materials Science Forum (Vol. 685). doi:10.4028/www.scientific.net/MSF.685.181

Meyer, C. (2009). The greening of the concrete industry. Cement and Concrete Composites, 31(8). doi:10.1016/j.cemconcomp.2008.12.010

Mouli, M., & Khelafi, H. (2008). Performance characteristics of lightweight aggregate concrete containing natural pozzolan. Building and Environment, 43(1). doi:10.1016/j.buildenv.2006.11.038

Özen, M., Demircan, G., Kisa, M., Acikgoz, A., Ceyhan, G., & Işıker, Y. (2022). Thermal properties of surface-modified nano-Al2O3/kevlar fiber/epoxy composites. Materials Chemistry and Physics, 278, 125689. doi: 10.1016/j.matchemphys.2021.125689

Peng, J., Huang, L., Zhao, Y., Chen, P., Zeng, L., & Zheng, W. (2013). Modeling of carbon dioxide measurement on cement plants. In Advanced Materials Research (Vol. 610–613). doi:10.4028/www.scientific.net/AMR.610-613.2120

Razak, R. A., Abdullah, M. M. A. B., Hussin, K., Ismail, K. N., Hardjito, D., & Yahya, Z. (2015). Optimization of NaOH molarity, LUSI mud/alkaline activator, and Na2SiO3/NaOH ratio to produce lightweight aggregate-based geopolymer. International Journal of Molecular Sciences, 16(5). doi:10.3390/ijms160511629

Sarmin, S. N. (2015). Lightweight building materials of geopolymer reinforced wood particles aggregate – A Review. Applied Mechanics and Materials, 802. doi:10.4028/www.scientific.net/amm.802.220

Shi, J., Liu, B., Liu, Y., Wang, E., He, Z., Xu, H., & Ren, X. (2020). Preparation and characterization of lightweight aggregate foamed geopolymer concretes aerated using hydrogen peroxide. Construction and Building Materials, 256. doi:10.1016/j.conbuildmat.2020.119442

Wongsa, A., Sata, V., Nuaklong, P., & Chindaprasirt, P. (2018). Use of crushed clay brick and pumice aggregates in lightweight geopolymer concrete. Construction and Building Materials, 188, 1025-1034.

Zhang, P., Zheng, Y., Wang, K., & Zhang, J. (2018). A review on properties of fresh and hardened geopolymer mortar. Composites Part B: Engineering. doi:10.1016/j.compositesb.2018.06.031

Zheng, Q., Kaur, S., Dames, C., & Prasher, R. S. (2020). Analysis and improvement of the hot disk transient plane source method for low thermal conductivity materials. International Journal of Heat and Mass Transfer, 151, 119331. doi: 10.1016/j.ijheatmasstransfer.2020.119331